Cerebral Cortex October 2015;25:3487–3501
doi:10.1093/cercor/bhu182
Advance Access publication August 21, 2014

Kalirin-9 and Kalirin-12 Play Essential Roles in Dendritic Outgrowth and Branching

Yan Yan[1], Betty A. Eipper[1,2] and Richard E. Mains[1]

[1]Department of Neuroscience, UConn Health, Farmington, CT 06030, USA and [2]Molecular Biology and Biophysics, UConn Health, Farmington, CT 06030, USA

Address correspondence to Richard E. Mains, Department of Neuroscience, UConn Health, 263 Farmington Avenue, Farmington, CT 06030, USA. E-mail: mains@uchc.edu

Proteins derived from the *Kalrn* gene, encoding 2 Rho guanine nucleotide exchange factor (GEF) domains, affect dendritic and axonal morphogenesis. The roles of endogenous Kalirin-9 (Kal9) and Kalirin-12 (Kal12), the *Kalrn* isoforms expressed before synaptogenesis, have not been studied in neurite growth and maturation during early development. The *Caenorhabditis elegans* and *Drosophila melanogaster* orthologues of *Kalrn* encode proteins equivalent to Kal9 but, lacking a kinase domain, neither organism expresses a protein equivalent to Kal12. Both in vivo and in vitro analyses of cortical neurons from total *Kalrn* knockout mice, lacking all major Kalirin isoforms, revealed a simplified dendritic arbor and reduced neurite length. Using isoform-specific shRNAs to reduce Kal9 or Kal12 expression in hippocampal cultures resulted in stunted dendritic outgrowth and branching in vitro, without affecting axonal polarity. Exposing hippocampal cultures to inhibitors of the first GEF domain of Kalirin (ITX3, Z62954982) blunted neurite outgrowth and branching, confirming its essential role, without altering the morphology of neurons not expressing *Kalrn*. In addition, exogenous expression of the active kinase domain unique to Kal12 increased neurite number and length, whereas that of the inactive kinase domain decreased neurite growth. Our results demonstrate that both endogenous Kal9 and endogenous Kal12 contribute to dendritic maturation in early development.

Keywords: Kalirin knockout mouse, kinase, neurite, Rho GEF

Introduction

Precise establishment of neural circuits requires appropriate axonal and dendritic morphogenesis (Craig and Banker 1994; Wong and Ghosh 2002; Jan and Jan 2010). Neuronal morphogenesis begins with axonal and somato-dendritic compartment formation. After several neurites arise from the cell body, higher-order neurites emerge from the primary neurites (Craig and Banker 1994; Konur and Ghosh 2005). Alterations in the normal formation of neuronal processes contribute to neurological and neurodevelopmental disorders such as schizophrenia, mental retardation, and autism (Pardo and Eberhart 2007; Van Maldergem et al. 2013; Xu et al. 2013).

Rho family GTPases are critical regulators of the actin cytoskeletal dynamics essential for neuronal morphogenesis (Nakayama et al. 2000; Tada and Sheng 2006). Guanine nucleotide exchange factors (GEFs) activate Rho proteins and are essential for process outgrowth and branching (Jaffe and Hall 2005; Miller et al. 2013). Kalirin, a multifunctional Rho GEF, contributes to dendritic and axonal morphology in several systems, as demonstrated through exogenous overexpression studies (May et al. 2002; Ma et al. 2003; Sommer and Budreck 2009). The *Kalrn* gene undergoes alternative splicing, generating isoforms with 1 [Kalirin-7 (Kal7)] or 2 [Kalirin-9 (Kal9) and Kalirin-12 (Kal12)] GEF domains (Fig. 1*A*): The first GEF domain (GEF1) activates RhoG and Rac1, whereas the second (GEF2) activates RhoA. Incorporation of 2 GEF domains into a single protein presumably allows coordinated regulation of signaling pathways controlling neurite outgrowth (Luo 2000a, 2000b; Penzes et al. 2001).

Much of our understanding of the role of dual Rho GEFs comes from studies of *Caenorhabditis elegans* and *Drosophila melanogaster*; *Unc-73* and *dTrio*, orthologues of *Kalrn* and *Trio*, the only other mammalian dual Rho GEFs, encode proteins equivalent to Kal9, but do not encode a protein kinase domain (Steven et al. 1998; Awasaki et al. 2000). *Unc-73* and *dTrio* play essential roles in axon guidance, but studies in these model organisms provide no insights into distinct functions that might be served by Kal9 and Kal12 in higher organisms. Interestingly, *Trio*, which also encodes a protein kinase domain, exhibits a different expression pattern and functions from *Kalrn* (Ma et al. 2005; McPherson et al. 2005; Peng et al. 2010; Miller et al. 2013).

Previous studies relied on overexpression of Kal9 and Kal12 to show that each can initiate fiber outgrowth in superior cervical ganglion neurons (May et al. 2002). Overexpression of Kal9 in cultured cortical neurons induces longer neurites and alters neuronal morphology (Penzes et al. 2001). However, the roles of endogenous Kal9 and Kal12 in early neuronal development, before Kal7 is expressed, are unclear. Studies on human subjects indicate a significant association between *KALRN* in one missense mutation ($P^{2255}T$, creating a potential phosphorylation site) and schizophrenia, which is unique to Kal9 and Kal12 (Hill et al. 2006; Kushima et al. 2012; Rubio et al. 2012). Thus, defining the roles of *KALRN* at different stages of development is of clinical and therapeutic importance. In this study, we focused on the earliest stages of neurite extension and dendritic branching, and found that endogenous Kal9 and Kal12 are required for dendrite formation both in vivo and in vitro. We also demonstrated distinct roles for Kal9 and Kal12, and for the putative kinase domain unique to Kal12.

Materials and Methods

Animals

$KalSR^{KO}$ mice were generated as described (Mandela et al. 2012) and have been back-crossed into the C57Bl/6 background (Jackson Laboratories, Bar Harbor, ME, USA) for >15 generations. All animals were housed in the UConn Health animal facility on a 12-h light/dark cycle with food and water ad lib. WT and $KalSR^{KO/KO}$ breeding units were maintained separately; $KalSR^{KO/KO}$ breeders are replaced frequently with mice obtained from $KalSR^{+/KO}$ breeding pairs, which are bred with WT mice (from Jackson Laboratories) every few months. $KalSR^{KO/KO}$ (referred to as $KalSR^{KO}$) animals exhibit deficits in nesting, pup rearing, and milk letdown (Mandela et al. 2012), so some pups were raised from P0 by WT females. All procedures were carried out in accord with the guidelines of the UConn Health Institutional Animal

© The Author 2014. Published by Oxford University Press. All rights reserved.
For Permissions, please e-mail: journals.permissions@oup.com

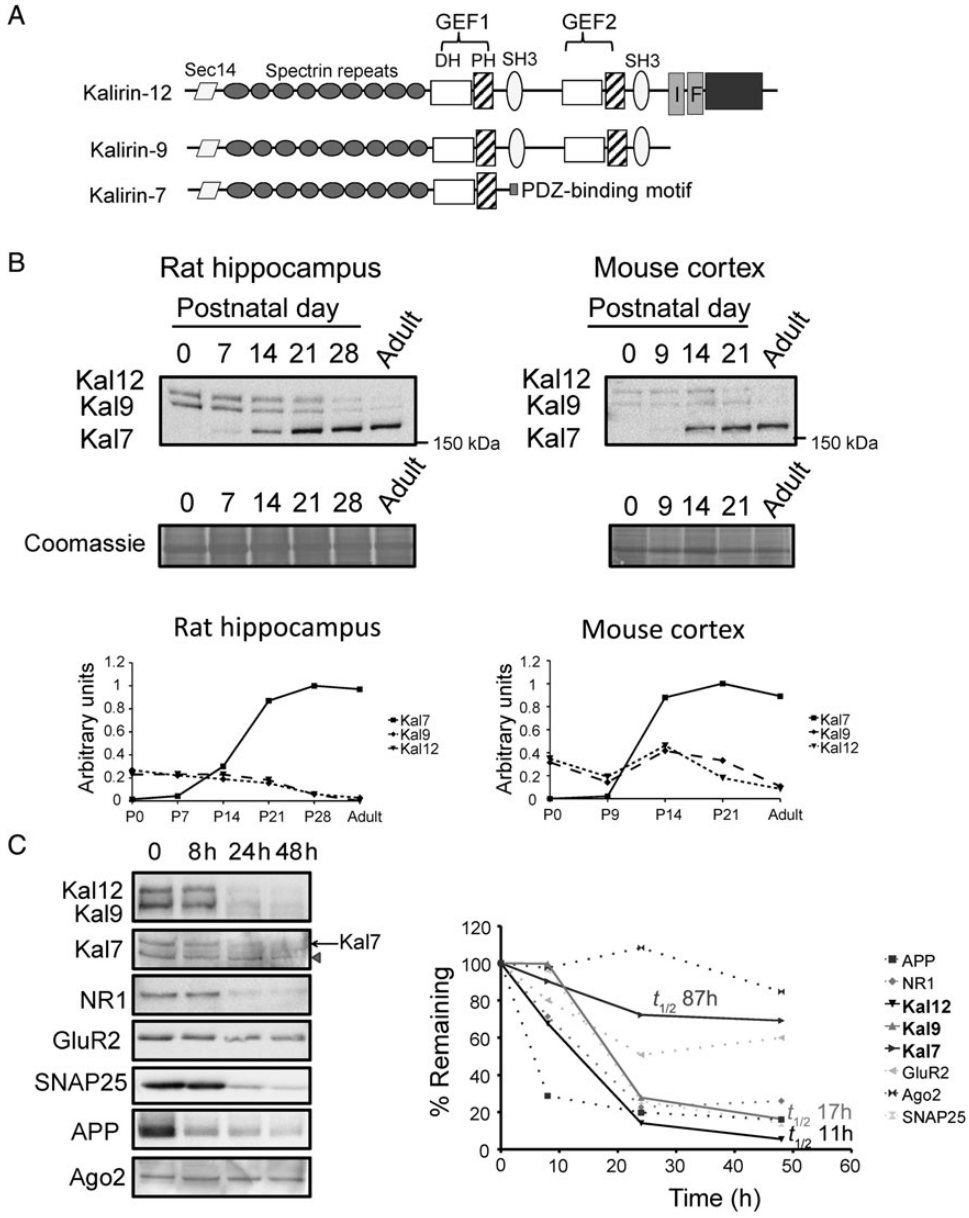

Figure 1. Developmental expression of Kalirin isoforms. (*A*) Diagram showing the major isoforms of Kalirin. (*B*) Rat hippocampi and mouse cortices were collected at the indicated ages; equal amounts of protein were subjected to western blot analysis and representative blots are shown. Affinity-purified Sec14 antibody was used to visualize all Kalirin isoforms. Below: quantification of Kal7, Kal9, and Kal12 after normalization to βIII tubulin; the maximum expression level was set to 1.0 for each data set; 3 sets of tissue were analyzed to generate both graphs. (*C*) Protein half-life was determined using cycloheximide (10 μM) to treat identical rat cortical cultures (DIV21) for the times indicated; lysates were subjected to western blot analysis. Loss of Kalirin was compared with loss of proteins known to turn over rapidly [APP (Morales-Corraliza et al. 2009), NR1 (Huh and Wenthold 1999)] or slowly [GluR2 (Huh and Wenthold 1999) and Ago2 (Adams et al. 2009)]. Ago2 turnover is rapid in cancer cells, but slow in neuronal cultures. Kal9 and Kal12 were detected using antibody CT301; Kal7 was detected using antibody JH2959. Arrowhead, known nonspecific band in Kal7 blot. Right: quantification of western blot signal as a function of time; half-lives for Kal7, Kal9, and Kal12 were calculated using semi-log plots. In parallel experiments using [^{35}S]Met to monitor protein synthesis in culture, 10 μM cycloheximide blocked 95% of protein synthesis, as expected (Sobota et al. 2009; not shown). This experiment was replicated 3 times with similar results.

Care and Use Committee. In addition to WT C57Bl/6 mice, KalSR$^{+/CKO}$ mice, which have a single floxed allele of *Kalrn* and exhibit no alterations from WT mice in behavioral or biochemical tests, were sometimes used as controls (Mandela et al. 2012).

Antibodies

Kalirin antibodies were described previously (Ma et al. 2003); JH2959 was used to detect Kal7. Antibodies to the Sec14 domain of Kalirin were produced by immunizing rabbits (Covance Research Products, Denver, PA, USA) with purified rat KalSec14 (NHDR … RLSL; pGEX4T2-KalSec14p); after ammonium sulfate precipitation, affinity purification was carried out using rat Sec14 linked to Affi-Gel15 beads. Affinity-purified CT301 and CT302 detect Kal7, Kal9, and Kal12. Commercial antibodies included: NR1 (N308/48, mouse, Neuromab); GluR2 (L21/32, mouse, Neuromab); amyloid precursor protein (APP; #51-2700, rabbit, Life Technologies, Carlsbad, CA, USA); Ago2 (#H00027161-M01, mouse, Novus Biologicals, Littleton, CO, USA); and SNAP25 (#610366, mouse, BD Biosciences, San Jose, CA, USA).

Cell Culture

Hippocampi from embryonic day 18 Sprague–Dawley rats were separated from telencephalic and diencephalic structures, and digested

with 0.28% trypsin for 15 min at 37 °C with gentle shaking. Cells were then dissociated with a fire-polished glass pipette. Freshly dissociated cells were nucleofected (Amaxa, Germany) using the rat neuron kit and program O-003. After nucleofection, neurons were plated at $\sim 30 \times 10^4$ cells/mL onto 12 mm coverslips coated with poly-L-lysine (1 mg/mL). Cells were plated in Dulbecco's Modified Eagle Medium: Nutrient Mixture F-12 (DMEM/F-12) containing 10% fetal calf serum, 5% heat-inactivated horse serum, 0.5 mM glutamine, 50 U/mL of penicillin, and 50 μg/mL of streptomycin and maintained at 37 °C in a 5% CO_2 atmosphere (all reagents were from Life Technologies). Twenty-four hours later, plating medium was replaced with Neurobasal medium containing 3% horse serum, 0.5 mM glutamine, 50 U/mL of penicillin, and 50 μg/mL of streptomycin. Thereafter, 50% of the culture medium was exchanged with Neurobasal medium containing 2% B27 supplement, 0.5 mM glutamine, 50 U/mL of penicillin, and 50 μg/mL of streptomycin twice a week. Cells were fixed at DIV2, DIV4, and DIV7 using 4% paraformaldehyde (PFA) in PBS. To examine the effects of Z62954982 (Millipore) and ITX3 (Sigma), a 10 000× stock of Z62954982 and a 1000× stock of ITX3 prepared in DMSO were diluted into growth medium to yield 10 μM Z62954982 and 100 μM ITX3 until harvest. DMSO was used in the vehicle group.

To conserve KalSR^{KO} mice, cultures were prepared from newborn pups; cortices were dissected from WT or KalSR^{KO} pups at P0 and dissociated and cultured at a low density (6×10^4/mL) as described above for hippocampi from E18 rat pups. Both rat and mouse neurons were stained with antisera to MAP2 (mouse, Sigma) or βIII tubulin (rabbit, Covance).

Knockdown and Overexpression Experiments

To reduce the expression of endogenous Kalirin in rat hippocampal cultures, shRNAs targeted to all major isoforms of rat Kalirin (Spec8 shRNA), the 3′UTR of Kal9 (Kal9 shRNA) and the kinase domain of Kal12 (Kal12 shRNA) were synthesized; the effects of shRNA-targeting *Kalrn* were compared with a control shRNA (scrambled shRNA), which matches nothing in rodent genomes or transcripts. To reduce endogenous Trio expression, an shRNA was designed to target its spectrin repeat region. Oligonucleotides were annealed and ligated into the RNAi-Ready-pSiren-DNR-DsRed-Express vector (Clontech, Mountain View, CA, USA). This vector places shRNA expression under control of the human U6 promoter and DsRed expression under control of the CMV promoter (Francone et al. 2010). The sequences targeted were: scramble shRNA, AATGCACGCTCAGCACAAGC; Spec8 shRNA, GCAGGAACAATGTGAGCATG; Kal9 shRNA, ACTGGACTGGACTTCTATT; Kal12 shRNA, CGATGAGCTGATGGAAGAA; Trio shRNA, TTCAGACGCAGCACAATCA. Transfection was performed at the time of plating using a Nucleofector™ 2b device (Lonza); 2.5×10^6 neurons were used for each transfection and the control (scramble) vector was used for each preparation of neurons. Each transfection included 2 μg of DNA encoding the indicated shRNA. In this study, up to 6 transfections were performed per neuronal preparation. For the rescue experiments, a larger amount of DNA was used; in addition to the shRNA vector (2 μg/transfection, Kal12 shRNA or Kal9 shRNA or control), 4 μg of the rescue vector (Kal9GFP or Kal12) was used to transfect 2.5×10^6 neurons. Neurons were fixed at DIV2, DIV4, or DIV7 as indicated.

Expression of exogenous Kalirin utilized existing pEAK10 vectors: ΔKal7 (Schiller et al. 2008); His-myc-tagged Kal9 and Kal12 (May et al. 2002); His-myc-tagged Kal-Kinase (^{2630}SEF—QGT^{2959}); His-myc-tagged Kal-Kinase (^{2630}SEF—QGT^{2959}) K^{2686}A, which is expected to be an inactive kinase due to the mutation in its putative ATP-binding site (prosite.expasy.org/cgi-bin/prosite/ScanView). All constructs were verified by sequencing. The GFP-farnesyl vector was used previously (Francone et al. 2010).

Experimental Treatment of Neuronal Cultures

To determine protein half-life, rat hippocampal neurons grown for 21 days in 12-well dishes (1×10^6 cells/well) were treated with cycloheximide (10 μM; EMD Millipore, Darmstadt, Germany) for the indicated length of time (Sobota et al. 2009). Cultures were harvested into SDS lysis buffer (0.5% SDS, 50 mM Tris, pH 8.0, 1 mM dithiothretiol, 1 mM phenylmethylsylfonyl fluoride, 2 mM EDTA, 50 mM NaF, 0.2 mM orthovanadate in the presence of lima bean trypsin inhibitor, pepstatin, leupeptin, and benzamidine) and used for western blot analysis as described below.

Immunocytochemistry and Image Acquisition

Immunocytochemical staining of neuronal cultures was performed as described (Ma et al. 2003). Images were taken using a Zeiss LSM 510 Meta confocal microscope and a 40× objective. For each neuron, neurite number and length were measured from the same image. Primary neurites that are longer than one soma diameter were counted at all days in vitro indicated.

Diolistic Labeling

Diolistic labeling was performed using a Gene Gun (Bio-Rad, Hercules, CA, USA) as described (Kiraly et al. 2010). Postnatal day 7 WT and KalSR^{KO} mouse pups were perfusion-fixed with 4% PFA followed by 1 h of postfixation in 4% PFA. Slices (150 μm) containing the prefrontal cortex were made using a vibratome (Leica, speed = 6^{70}; frequency = 8). DiI-coated gold particles were prepared using 0.125 mg DiI (Molecular Probes) and 50 mg of 1.0 μm gold microcarriers (Bio-Rad). After diolistic labeling, the dye was allowed to fill the processes (overnight) before imaging. Slides were counterstained with 1 μM TO-PRO-3 (Invitrogen) to visualize the cortical layers. Images were taken using a Zeiss LSM 510 Meta confocal microscope; Z-stacks (1 μm steps) of 40–50 μm were collected. Collapsed images of layer V pyramidal neurons (diameter 20–45 μm) were analyzed for dendrite number and Sholl analysis was performed (May et al. 2002).

Western Blot Analysis

For time course studies, cortices and hippocampi collected from rats and mice, respectively, of different ages were sonicated into the SDS lysis buffer used for half-life studies, heated for 5 min at 95 °C, and centrifuged to remove insoluble debris. The concentration of protein in the supernatant was determined using the bicinchoninic acid assay (Pierce, Rockford, IL, USA) with bovine serum albumin as a standard; 20 μg of total protein was loaded onto each lane for analysis of Kalirin expression. For the cycloheximide experiment, 1/10 of the total sample was loaded on the gel.

Results

Developmental Changes in Kalirin Isoform Expression in Rat and Mouse CNS

Since we wished to take advantage of previous studies on dissociated rat hippocampal neurons and also wished to use both KalSR^{KO} mice and dissociated KalSR^{KO} cortical neurons, we first evaluated Kalirin isoform expression in rat hippocampus and mouse cortex during early postnatal development. We developed a new antibody directed to the Sec14 domain, which is present in all of the full-length Kalirin isoforms (Fig. 1*A*), allowing comparison of levels of Kal7, Kal9, and Kal12 at various ages. Western blot analysis of P0 extracts from rat hippocampi and mouse cortices revealed the expression of similar amounts of Kal9 and Kal12, with no detectable Kal7 (Fig. 1*B*). In the adult hippocampus and cortex a switch occurs, with Kal7 the major isoform and low, but similar levels of Kal9 and Kal12. In both rat hippocampus and mouse cortex, expression of Kal7 was first detectable between P7 and P14 and peaked between P21 and P28 (Fig. 1*B*). The early prevalence of Kal9 and Kal12 in both rat hippocampus and mouse cortex is consistent with a role for these isoforms in neurite outgrowth, polarity establishment, and dendrite formation.

To eliminate selectively Kal9 or Kal12 expression in neuronal cultures, we chose shRNA-encoding vectors. Protein half-life determines the length of time required before an effect on

function can be expected. To assess the half-lives of Kal7, Kal9, and Kal12, we added 10 μM cycloheximide, a protein synthesis inhibitor (Sobota et al. 2009), to cultured rat neurons and evaluated protein levels as a function of treatment time (Fig. 1*C*). When densitized values for Kal7, Kal9, and Kal12 expression were plotted on a semi-log scale, data for each could be fit to a single straight line, suggesting an exponential decay process. The half-lives calculated for Kal9 (17 h) and Kal12 (11 h) were clearly shorter than the half-life for Kal7 (87 h), while very short half-life proteins (APP) and very long-lived proteins (GluR2 and Ago2) behaved as expected (Huh and Wenthold 1999; Adams et al. 2009; Morales-Corraliza et al. 2009). Based on this information, we transfected dissociated E18 rat hippocampal neurons at the time of plating and evaluated morphological changes in response to manipulations of Kalirin levels between DIV2 and DIV7.

Dendritic Alterations in KalSR^{KO} Cortex In Vivo

Based on our developmental time course studies, we sacrificed WT and KalSR^{KO} mice at postnatal day 7, when Kal9 and Kal12 are the major *Kalrn* isoforms expressed. No gross anatomical changes were detected in KalSR^{KO} brains and the 6-layer lamination of the neocortex was intact and indistinguishable from WT (Fig. 2*A*,*B*). To explore whether the absence of Kal9 and Kal12 altered neuronal morphology in vivo, we performed diolistic labeling using lightly fixed brain slices from P7 WT or KalSR^{KO} pups (Shen et al. 2009; Kiraly et al. 2010). The fine morphology of neocortical pyramidal neurons was visualized using DiI, a lipophilic dye; collapsed Z-stack confocal images of isolated DiI-filled neurons were selected for analysis (Fig. 2*C*). We focused on layer V, which contains the large pyramidal neurons that are the major intracortical and subcortical output neurons (Petreanu et al. 2009). Layer V neurons receive

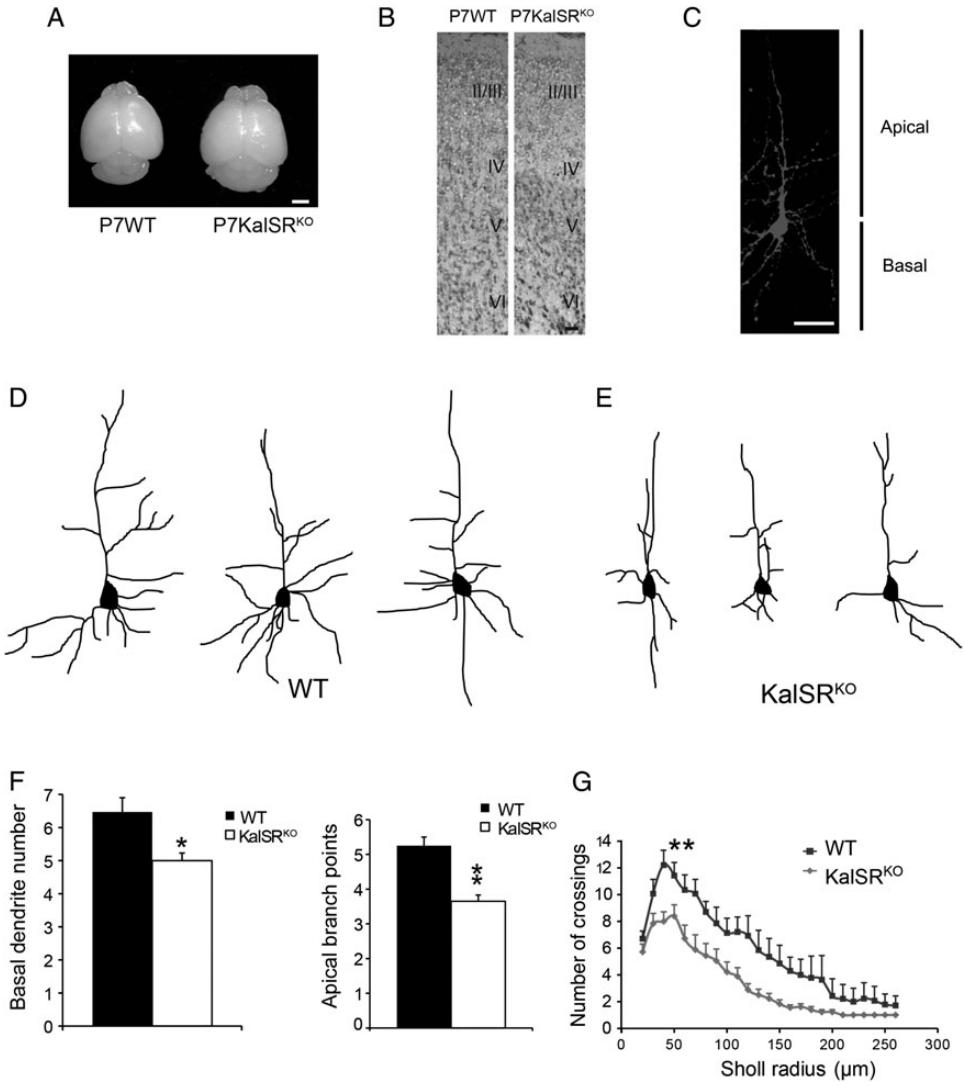

Figure 2. Neuronal morphology is altered in layer V cortical neurons in postnatal day 7 KalSR^{KO} mice. (*A*) Dorsal view of P7 WT and KalSR^{KO} brains. (*B*) Cresyl violet staining of coronal slices through the prefrontal cortex of WT and KalSR^{KO} animals. (*C*) Representative collapsed Z-stack confocal image of DiI-labeled WT cortical layer V neuron. (*D* and *E*) Camera lucida drawings of representative layer V pyramidal neurons from WT or KalSR^{KO} cortices. (*F*) Quantification of basal dendrite number and apical branch points in DiI-labeled layer V cortical neurons; 26 WT and 30 KalSR^{KO} neurons from 8 animals were analyzed. *$P < 0.05$; **$P < 0.01$. (*G*) Sholl analysis was performed on DiI-labeled neurons using 22 WT neurons and 24 KalSR^{KO} neurons. Concentric circles (radius 20–260 μm) were drawn around each cell soma; the number of intersections with neurites extending from that soma was counted for each circle. **$P < 0.01$. Two-way ANOVA with Bonferroni post-tests. Scale bar: 1 mm in *A*; 50 μm in *B* and *C*.

inputs from all of the cortical layers via their extensive basal and apical dendrites.

We first compared the basal compartment and found that KalSR^{KO} neurons exhibited a poorly branched basal dendritic arbor (Fig. 2*D*,*E*). The number of basal dendrites per cell was diminished in KalSR^{KO} layer V neurons (Fig. 2*F*; WT, 6.5 ± 0.43; KalSR^{KO}, 5.3 ± 0.25; $N = 26–29$; $P < 0.02$). Examination of the apical dendrites of layer V KalSR^{KO} neurons revealed that some failed to reach the upper cortical layers, unlike the apical dendrites of WT controls (data not shown). Quantification of apical branch points revealed a significant decrease in KalSR^{KO} neurons compared with control neurons (WT, 5.3 ± 0.25; KalSR^{KO}, 3.7 ± 0.18; $N = 22–25$; $P < 0.01$; Fig. 2*F*). Sholl analysis showed a reduction of crossing number in KalSR^{KO} neurons (Fig. 2*G*), suggesting a simplified dendritic branching pattern. Taken together, our data indicate that *Kalrn* plays an important role in the early stages of neuronal morphogenesis, before Kal7 is expressed and before dendritic spines are formed. To investigate the actions of endogenous Kal9 and Kal12 in early development, we turned to dissociated neuronal cultures.

Kal9 and Kal12 are necessary for dendrite formation and branching in vitro, but do not affect axon specification.

Endogenous Kalirin expression in hippocampal neurons was diminished using an shRNA (Spec8 shRNA) targeting the spectrin 8 region, which is present in both Kal9 and Kal12 (Fig. 3*A*). The efficiency of the Spec8 shRNA was verified using a mycΔKal7 expression vector in pEAK Rapid cells (Fig. 3*A*).

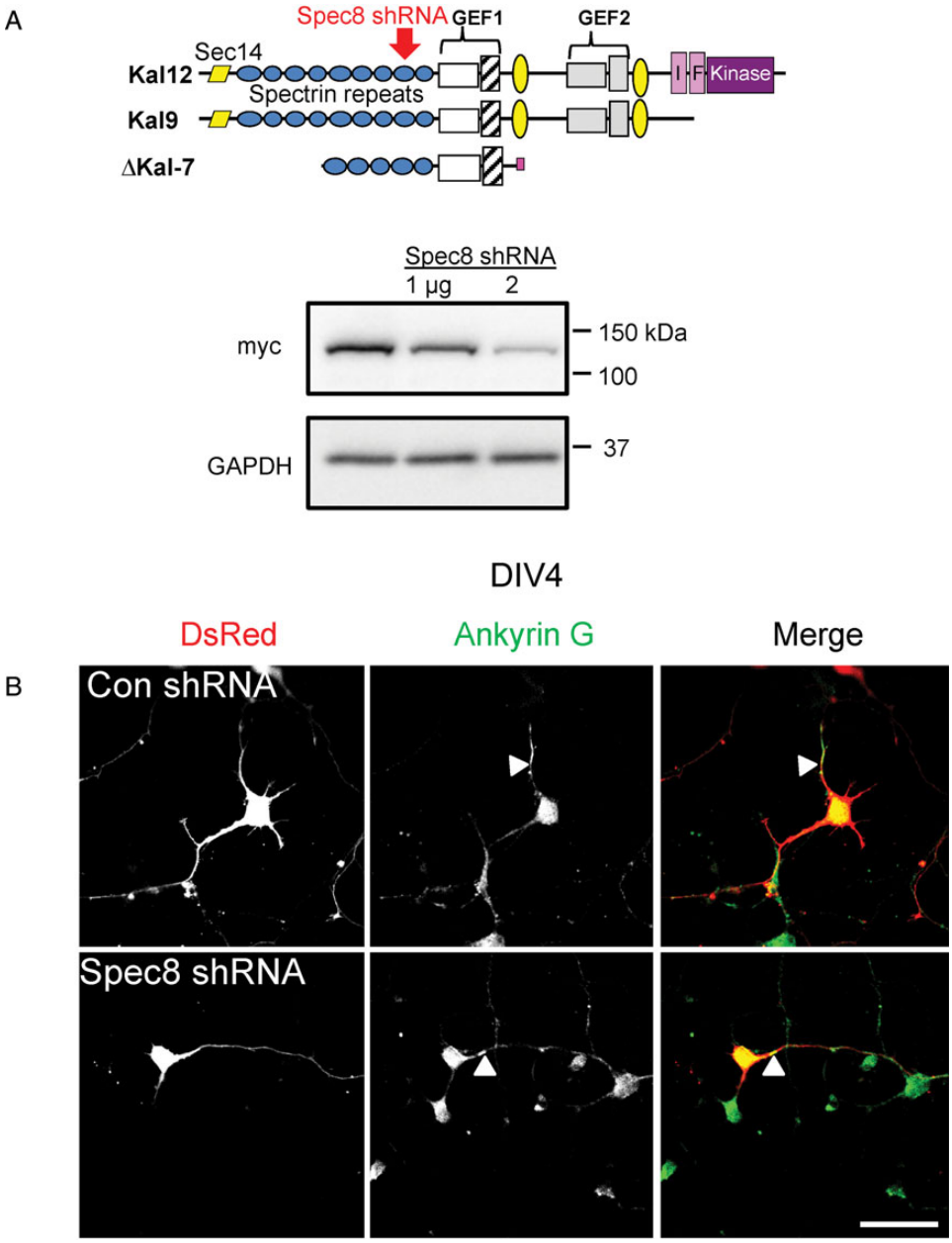

Figure 3. Kal9 and Kal12 do not affect axon polarity. (*A*) pEAK Rapid cells co-transfected with vectors encoding mycΔKal7 and Spec8 shRNA (1 or 2 µg, as indicated) were harvested after 24 h; the site targeted by this shRNA is shown. Western blot analysis using a myc antibody demonstrated a dose-dependent decrease in mycΔKal7 expression. (*B*) Examples of DIV4 hippocampal neurons transfected at plating with control or Spec8 shRNA and stained for Ankyrin G (green). Scale bar: 50 µm.

At the time of plating, dissociated hippocampal neurons were nucleofected with either Spec8 shRNA to suppress both Kal9 and Kal12 expression, or a scramble shRNA control (Yan et al. 2013); co-expression of DsRed allowed identification of shRNA-expressing neurons and assessment of their morphology. Cultures from embryonic hippocampal neurons have been widely used as a model system to study neuronal development (Craig and Banker 1994). After plating, neurons initially form a lamellipodium (stage 1), followed by several short neurites that seem identical to each other (stage 2). After about 2 days, one neurite extends rapidly and becomes the axon (stage 3; Dotti et al. 1988). To determine whether *Kalrn* plays a role in axon formation, we used an antibody to Ankyrin G, which localizes to the axon initial segment (Zhou et al. 1998), to identify axons after DIV4. Ankyrin G staining at DIV4 and DIV7 revealed a single axon in both groups (1.0 ± 0 Ankyrin G-positive neurites/neuron; Fig. 3*B*), suggesting that axon polarity can be generated normally in the absence of *Kalrn*.

Next, we examined dendrite formation. Compared with control neurons, expression of Spec8 shRNA significantly reduced both the number of primary dendrites and the number of branch points at DIV4 and at DIV7 (Fig. 4*A*,*B*). The effect of expressing Spec8 shRNA on the dendritic branching pattern was confirmed by Sholl analysis, with a reduction in crossing number apparent at DIV4 and at DIV7 (Fig. 4*C*,*D*).

To further confirm a role of endogenous *Kalrn* in dendrite formation, we asked whether a similar deficit could be observed in KalSR^{KO} cortical neurons in vitro. Neurons were stained for MAP2 to enable morphological quantification. Consistent with the shRNA knockdown experiments in hippocampal neurons, KalSR^{KO} cortical neurons had fewer primary dendrites and fewer branch points than WT cortical neurons (Fig. 4*E*,*F*). Sholl analysis at DIV4 and DIV7 confirmed a reduction of crossing number in the KalSR^{KO} cortical neurons (Fig. 4*G*,*H*). Taken together, our experiments demonstrate that the isoforms of *Kalrn* expressed early in development (Kal9 and Kal12) play an essential role in dendritic outgrowth and branching in both rat hippocampal and mouse cortical neurons, without affecting axon polarity. Next, we wished to explore the underlying mechanisms involved.

Kal GEF1-Mediated Rac1 Activation Is Required for Neurite Formation

We employed pharmacological tools to evaluate the role of Kal GEF1-activated Rac1 in neurite morphogenesis. Z62954982 was designed as a cell permeant inhibitor of the interaction of Rac1 with several of its GEFs and is not specific for Kal GEF1 (Ferri et al. 2009). ITX3 is a cell permeable inhibitor specific for the GEF1 domains of Kalirin and Trio (Bouquier et al. 2009), which are >90% identical (McPherson et al. 2002). The inhibitor or the vehicle control (DMSO) was added 4 h after plating and neurons were fixed at DIV2. To visualize neuronal morphology, neurons were transfected with control shRNA as described in Figure 4 or with membrane-targeted GFP (GFP-farnesyl). Two methods of visualization were used in case one was deleterious to the neurons.

Neurons treated with the Rac1 activation inhibitor, Z62954982, showed a significant decrease in both the number of neurites and branch points at DIV2 (Fig. 5*A*–*C*), suggesting that Rac1 activation is essential for neurite formation; similar results were obtained using both methods of visualizing isolated neurons. Neurons treated with the Kalirin/Trio GEF1 inhibitor, ITX3, showed a similar reduction in the number of primary neurites and branch points (Fig. 5*A*–*C*), suggesting that Kal GEF1 activity is essential for neurite development. The fact that both inhibitors exerted similar effects on neurite number and branch point number suggests that ITX3-sensitive GEFs are responsible for activating the Rac1 that participates in these processes. Since transfection with an shRNA targeted to *Trio* did not produce a decrease in neurite number or branching, it is unlikely that the GEF1 domain of Trio is responsible for Rac1 activation in these cultures (Figs 3 and 4; data not shown). Taken together, these results suggest that the ability of the GEF1 domain of endogenous Kal9 and/or Kal12 to activate Rac1 is required for normal neurite development. To rule out any off-target effects on the pharmacological inhibitors, we applied either ITX3 or Z62954982 to KalSR^{KO} cultures. Neither ITX3 nor Z62954982 produced a statistically significant change in the number of primary neurites or branch points (Fig. 5*D*, *E*), suggesting that Kalirin plays a major role among other GEFs in early dendritic arbor development. Next, we wished to determine whether Kal9 and Kal12 were redundant or each played an essential role in neurite development.

Functions of Endogenous Kal9 and Kal12 Are Distinguishable

To study the roles of Kal9 and Kal12 separately, we designed shRNAs that target a region unique to each transcript (Fig. 6*A*). Kal12 shRNA efficiency and specificity were verified by co-transfection of pEAK Rapid cells with a Kal12 or Kal Kinase expression vector and the Kal12 shRNA vector (Fig. 6*A*). For Kal12, western blot analysis was carried out using an antibody specific for myc; expression of Kal12 and Kal Kinase were reduced to 10–20% of control in the presence of the Kal12 shRNA. We could not directly verify the Kal9 shRNA efficiency because this shRNA targeted the Kal9 3′UTR, the only unique region, which is not present in our expression vectors.

Rat hippocampal neurons transfected at the time of plating with Kal9 or Kal12 shRNA were evaluated at DIV2, DIV4, and DIV7 (Fig. 6*B*–*D*). We quantified the number of primary neurites and the number of branch points. Compared with the control (Scr) shRNA, expression of either the Kal9 or Kal12 shRNA resulted in a decrease in the number of primary neurites and in the number of branch points at each time (Fig. 6*D*); the effect of the Kal9 shRNA did not differ from that of the Kal12 shRNA and neither had a great effect at DIV7 as the Spec8 shRNA. These results suggest that Kal9 and Kal12 are both involved in the formation of dendritic arbor. To rule out any off-target shRNA phenotypes, we tried to reverse the knockdown phenotype by co-expressing the Kal9 shRNA with a vector encoding Kal9GFP, a fusion protein (Fig. 6*E*,*F*). This shRNA targets the 3′UTR of Kal9, which is not included in the Kal9GFP expression vector. Neurons expressing both DsRed (Kal9 shRNA) and GFP (Kal9GFP) were evaluated to assess rescue; neurons from the same transfection that expressed Kal9GFP but not DsRed were also evaluated to assess the effect of overexpressing Kal9GFP. We did not observe a statistically significant difference in the number of primary neurites and branch points between neurons expressing the control (Scr) shRNA and neurons expressing Kal9GFP (Fig. 6*D*,*F*). At both DIV4 and DIV7, neurons co-expressing the Kal9 shRNA and Kal9GFP exhibited more neurites and more branch points than

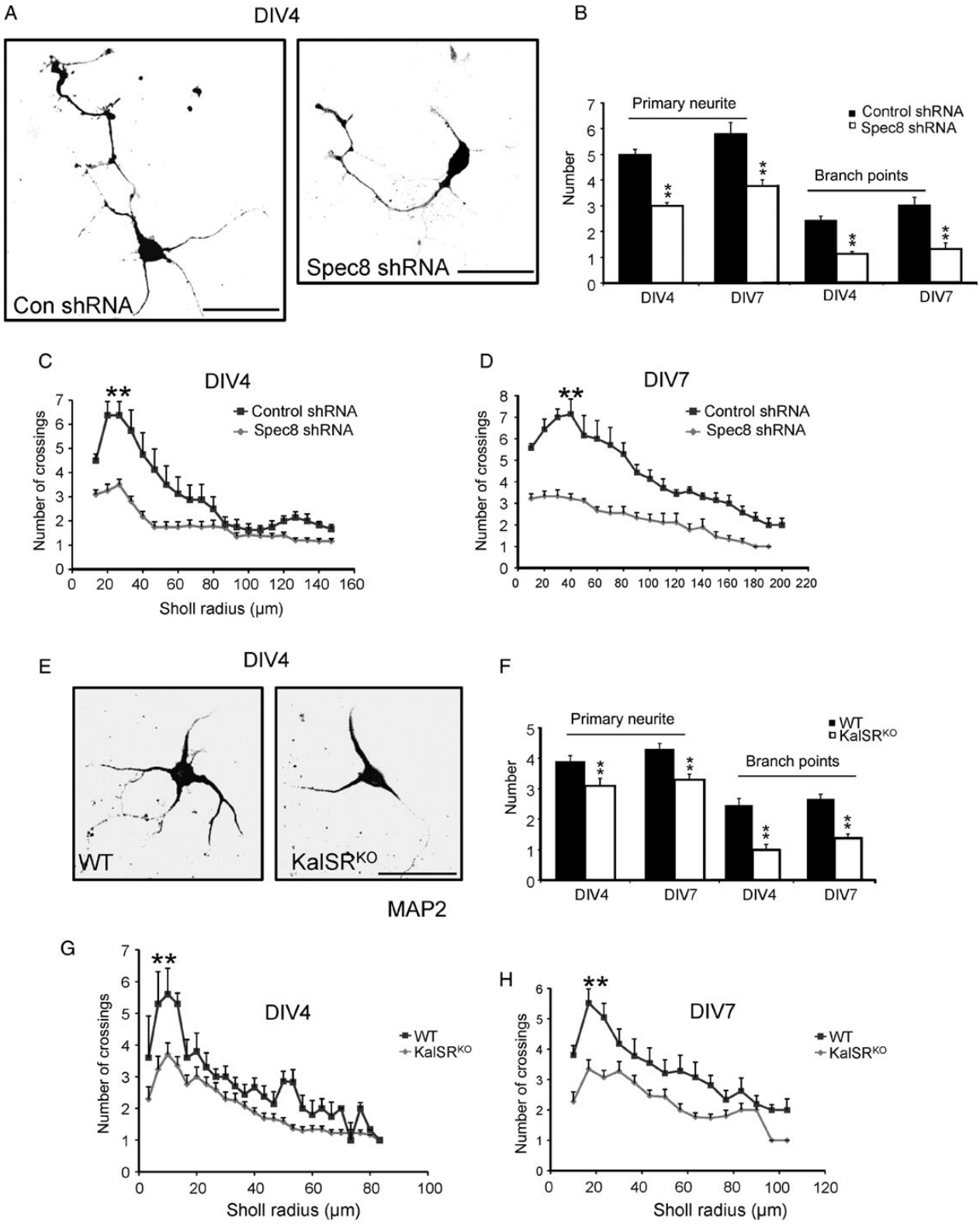

Figure 4. Kal9 and Kal12 are necessary for dendrite formation and branching, respectively. (*A*) Rat hippocampal neurons nucleofected at the time of plating with a control (scrambled) shRNA or Spec8 shRNA were fixed and analyzed at the indicated times. shRNA-transfected neurons were visualized using DsRed; images were converted to black and white for ease of morphological comparison. (*B*) Quantification of primary neurites and branch points. At both DIV4 and DIV7, neurons expressing Spec8 shRNA exhibited fewer primary neurites and fewer branch points than that expressing the control shRNA. Six separate experiments were performed; 20–30 neurons per group per experiment were counted. $^{**}P < 0.01$. Scale bar: 50 μm. (*C* and *D*) Sholl analysis was carried out for DIV4 and DIV7 neurons as described in Figure 2; $^{**}P < 0.01$. The processes of Spec8 shRNA-expressing neurons had significantly fewer intersections than that of control neurons. (*E*) Cortical neurons from WT or KalSR^{KO} mice were maintained in culture until DIV4; cultures were fixed and stained with a MAP2 antibody to visualize neurites. Scale bar: 50 μm. (*F*) Primary neurites and branch points in WT and KalSR^{KO} neurons were quantified as described above; 3 separate experiments were carried out; 15–23 neurons per group per experiment were analyzed. $^{**}P < 0.01$. (*G* and *H*) Sholl analysis was carried out on WT and KalSR^{KO} neurons as described above at DIV4 and DIV7; $^{**}P < 0.01$.

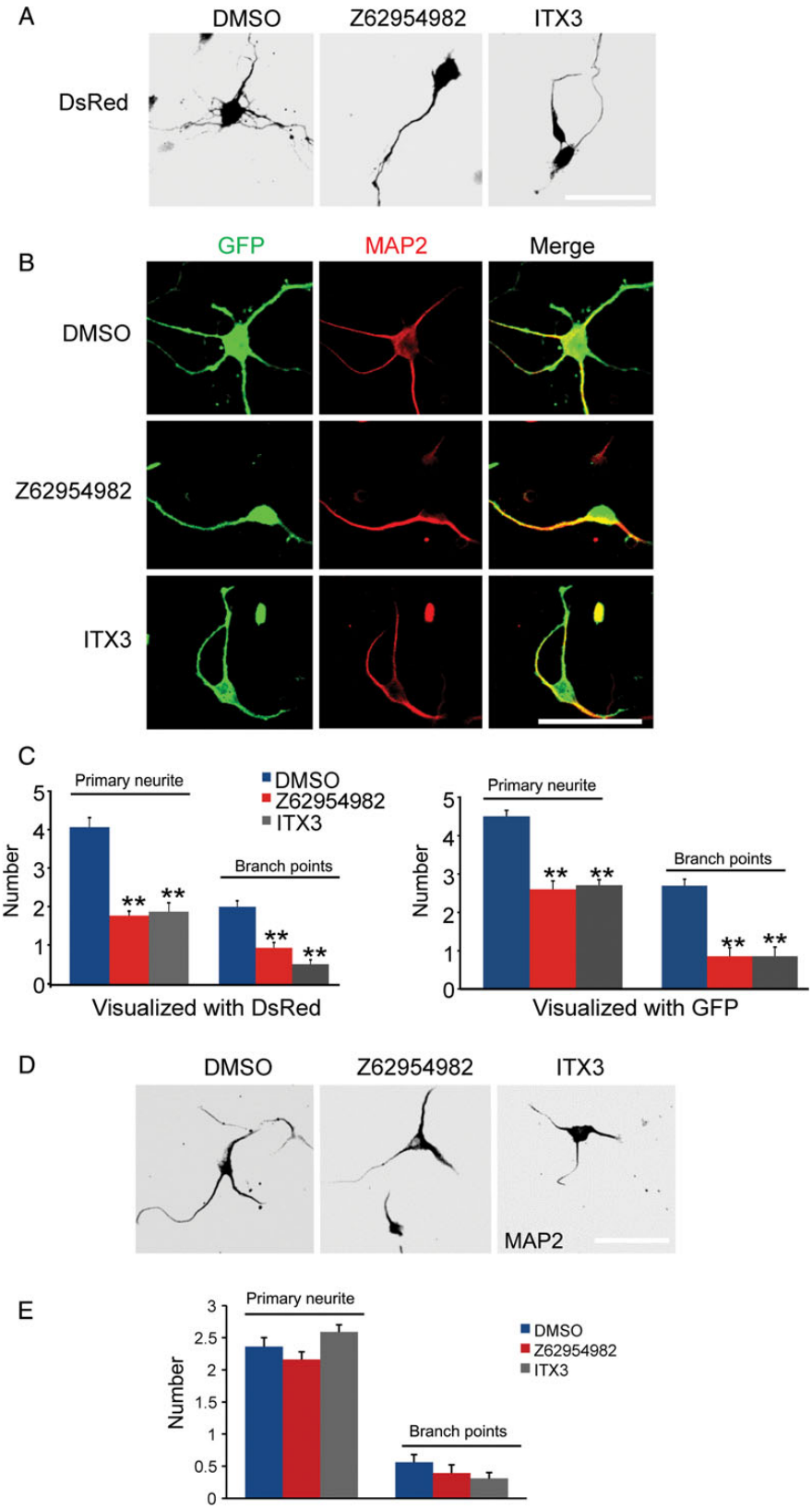

Figure 5. Kalirin GEF1-mediated Rac1 activation is essential for neurite formation. (*A*) Hippocampal neurons were transfected with control shRNA at the time of plating and were kept in the presence of DMSO (vehicle), Rac1 activation inhibitor (Z62954982), or Kalirin/Trio GEF1 inhibitor (ITX3) until fixation at DIV2. (*B*) Hippocampal neurons were transfected with farnesyl-GFP at the time of plating and were kept in the presence of vehicle or the indicated inhibitor until fixation at DIV2; fixed cells were stained for MAP2 (red). Scale bar: 50 μm. (*C*) Quantification of the effect of Rac1 activation inhibitor and Kalirin/Trio GEF1 inhibitor on primary neurite and branch point number. $^{**}P < 0.01$. (*D*) Representative images of MAP2 stained KalSR^{KO} neurons at DIV2, in the presence of DMSO (vehicle), Z62954982, or ITX3. Scale bar: 50 μm. (*E*) Quantification of effect of Rac1 activation inhibitor and Kalirin/Trio GEF1 inhibitor on KalSR^{KO} neurons at DIV2. Two separate experiments were carried out; 12–16 neurons per group per experiment were analyzed; neither inhibitor had a significant effect on primary neurite number or branch point number in KalSR^{KO} neurons.

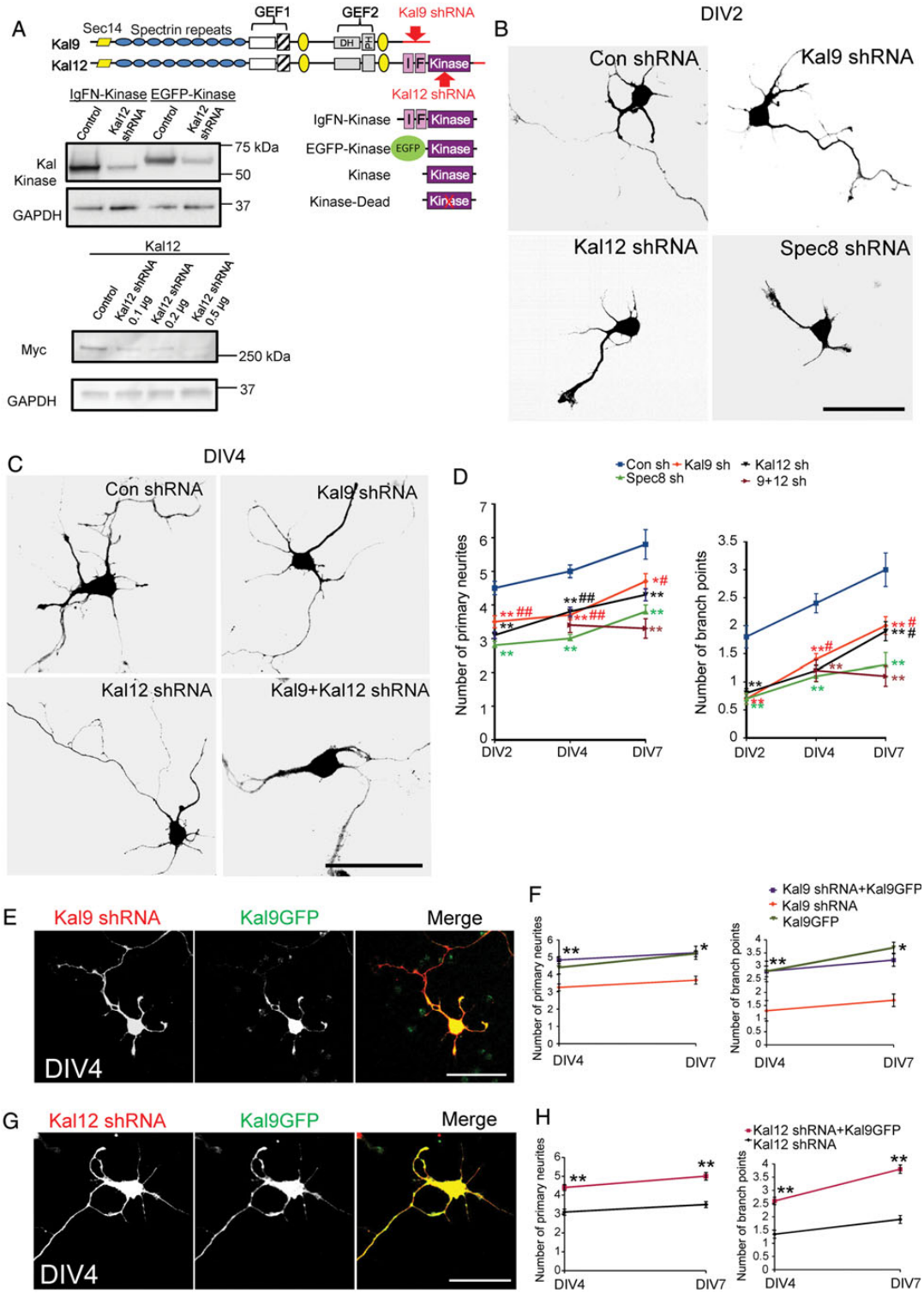

Figure 6. Functions of Kal9 and Kal12 are distinguishable. (*A*) Diagram of shRNAs targeting transcripts encoding Kal9 and Kal12; the Kal9 shRNA targets a site in the 3′-untranslated region. The proteins encoded by the Kal Kinase expression vectors are shown. Below: pEAK Rapid cells co-transfected with vectors encoding IgFN-Kal Kinase or EGFP-Kal Kinase (1 µg kinase vector and 1 µg control or Kal12 shRNA vector). The same cells were transfected with vectors encoding Kal12 (2 µg) and the Kal12 shRNA (0.1, 0.2, or 0.5 µg) and extracted 24 h later. (*B*) Examples of rat hippocampal neurons transfected at the time of plating with control (Scr) shRNA, Kal9 shRNA, Kal12 shRNA, or Spec8 shRNA; cultures were fixed at DIV2 and neurite number and branching were evaluated. (*C*) Hippocampal neurons co-transfected with control (Scr), Kal9 shRNA, Kal12 shRNA, or a mixture containing both Kal9 and Kal12 shRNAs were visualized in the same manner at DIV4; all cultures received 2 µg shRNA vector. (*D*) Summary of data for primary neurite and branch point number in hippocampal neurons expressing the indicated shRNAs for different periods of time. $^{*}P < 0.05$, $^{**}P < 0.01$ to control shRNA; $^{\#}P < 0.01$, $^{\#\#}P < 0.05$ to Spec8 shRNA. Quantification used data pooled from 5 to 9 separate experiments (including Kal9GFP rescue experiments); 24–69 neurons per group per experiment were analyzed. (*E*) Representative images of DIV4 neurons co-transfected with Kal9 shRNA and Kal9GFP. (*F*) Quantification of Kal9GFP alone (no DsRed), Kal9 shRNA, and Kal9GFP/Kal9 shRNA co-transfected neurons at DIV4 and DIV7. $^{*}P < 0.05$. Kal9GFP alone data from the Kal9 shRNA + Kal9GFP and Kal12 shRNA + KalGFP experiments were pooled. (*G*) Representative images of DIV4 neurons transfected with Kal12 shRNA and vector encoding Kal9GFP fusion protein. Scale bar: 50 µm. (*H*) Quantification of Kal12 shRNA and Kal9GFP/Kal12 shRNA co-transfected neurons at DIV4 and DIV7. $^{*}P < 0.05$. Four separate experiments were conducted; 13–25 neurons per group per experiment were analyzed.

that expressing the Kal9 shRNA (Fig. 6*E*); neurons expressing both the Kal9 shRNA and Kal9GFP resembled neurons expressing Kal9GFP (Fig. 6*F*). We attempted to co-express Kal12 shRNA and Kal12GFP; the low efficiency at which Kal12GFP, a 350-kDa protein, was expressed precluded analysis.

To see if their effects were additive, the Kal9 and Kal12 shRNAs were co-transfected; at DIV7, expression of both shRNAs had a greater effect than that of either individual shRNA and was comparable to the effect of the Spec8 shRNA (Fig. 6*C*, *D*). Additional information on the extent to which each shRNA reduces expression of its target protein and the time course of the knockdown effect will be needed to interpret fully the results of the co-transfection experiment.

Based on western blot analysis of neonatal tissue, Kal9 and Kal12 are expressed at similar levels during the time period under study (Fig. 1*B*). To determine whether expression of Kal9 could at least partially compensate for a decrease in Kal12 expression (in neurite production and branching), we co-expressed the Kal12 shRNA with the plasmid encoding Kal9GFP (Fig. 6*G*,*H*). Neurons expressing both the Kal12 shRNA and Kal9GFP and that expressing only Kal9GFP (no DsRed) were evaluated; data for neurons expressing Kal9GFP alone were pooled from the Kal9 shRNA and Kal12 shRNA rescue experiments. When assessed at DIV4 or at DIV7, it was clear that expression of Kal9GFP increased neurite complexity in cells expressing Kal12 shRNA (Fig. 6*B–D*); the morphology of neurons expressing Kal12 shRNA and Kal9GFP resembled that of Kal9GFP and control (Scr) shRNA-expressing neurons (Fig. 6*B–D*,*E*). These overexpression studies suggest that endogenous Kal9 and Kal12 have distinct, but overlapping functions; better control of Kal9 and Kal12 expression levels will be required to distinguish their roles during early development.

Another important aspect of neuronal morphology is neurite length. To see if we could distinguish the effects of endogenous Kal9 and Kal12 on this parameter, we measured total neurite length and the length of the longest neurite in neurons expressing shRNAs targeted to Kal9, Kal12, or all Kalirin isoforms; after DIV2, the longest neurite is presumably the axon. Consistent with the Sholl analyses presented for rat hippocampal neurons in Figure 4, expression of the Spec8 shRNA reduced both total neurite length and the length of the longest neurite in rat hippocampal neurons (Fig. 7*A*). At both DIV2 and DIV7, expression of Kal9 or Kal12 shRNA decreased neurite length, but not to the same extent as that of Kal8 shRNA; the same amount of shRNA vector was used in each case (Fig. 7*A*). Consistent with the shRNA experiments in rat neurons, KalSR^{KO} mouse neurons exhibited a decrease in total neurite length and in the length of their longest neurite when compared with WT neurons at DIV5 (not shown) and DIV7 (Fig. 7*B*). These results suggest that endogenous Kal9 and Kal12 are both involved in neurite outgrowth and contribute to dendritic and axonal length.

Expression of Exogenous Kal Kinase Alters Neuronal Morphology

To determine whether Kal12 plays a role in neurite morphogenesis that cannot be played by Kal9, we next investigated the function of the Ser/Thr kinase domain unique to Kal12 (Fig. 6*A*). We expressed exogenous myc-tagged Kal Kinase or GFP in rat hippocampal neurons at the time of plating, and found that neurons expressing Kal Kinase had a distinctly different morphological appearance, with more primary neurites and branch points at DIV2 and at DIV4 than control neurons (Fig. 8*A*,*B*). Measurement of total neurite length and the longest neurite revealed a significant increase in both parameters in neurons expressing Kal Kinase at DIV4 (Fig. 8*C*). The effect of exogenous Kal Kinase on total neurite length was more dramatic than its effect on the longest neurite.

Although autophosphorylation of Kal Kinase has been demonstrated (Kawai et al. 1999), no other Kal Kinase substrates have been identified. Comparison to other Ser/Thr kinases allowed identification of the putative ATP-binding site in Kal Kinase (K^{2686}). To render the kinase inactive, we mutated K^{2686} to A^{2686} (Caldwell et al. 1999). Neurons expressing Kal Kinase/K^{2686}A resembled neurons expressing Spec8 shRNA (Fig. 8*A*,*B*). The number of primary neurites and of branch points in neurons expressing the mutated kinase were both reduced below control levels, suggesting that the inactive kinase acts as a dominant negative; the effect of expressing Kal Kinase/K^{2686}A appeared to be greater than that of reducing the expression of endogenous Kal12. Taken together, our results suggest that the kinase domain of Kalirin plays a crucial role in neuronal process outgrowth, and that its ability to do so requires its catalytic activity.

To determine whether exogenous Kal Kinase functions independently or can only act through an interaction with endogenous Kalirin, we expressed exogenous Kal Kinase in KalSR^{KO} neurons. Expression of the Kal Kinase domain produced a dramatic increase in the number of primary neurites and branch points when assessed at DIV4 (Fig. 8*D*,*E*). The Kal Kinase expressing KalSR^{KO} neurons showed similar morphology to WT neurons at DIV4 (Fig. 6*E*). These results indicate that Kal Kinase promotes neurite outgrowth and branching independent of endogenous Kal9 and Kal12, and suggest that endogenous Kal12 serves some roles that cannot be fulfilled by Kal9.

Discussion

In the current study, we provided compelling evidence that endogenous Kal9 and Kal12 are essential to dendritic outgrowth and branching in early development both in vivo and in vitro. More importantly, we discovered that the Kal Kinase domain and its catalytic activity contribute to dendritic morphogenesis. Using the newly developed Kalirin Sec14 antibody, we compared the expression of all full-length isoforms at different ages in both rat and mouse. The longer *Kalrn* isoforms (Kal9 and Kal12) were the only ones expressed early in development; Kal7 appeared later, as observed for other postsynaptic markers, and became the major isoform only after P21 (Fig. 1*A*,*B*).

Both Kal9 and Kal12 Play Essential Roles

The different time course for the expression of Kal7 and Kal9/Kal12 made it straightforward to appreciate the unique roles of the isoforms with 2 Rho GEF domains in early development. We demonstrated distinct roles for endogenous Kal9/Kal12 in rodent using shRNAs and knockout animals. Developmental defects associated with the absence of Kal9/Kal12 were revealed by examining the cortex of early postnatal KalSR^{KO} mice; although axonal length was not evaluated, it was clear that formation of both apical and basal dendrites was diminished. Using

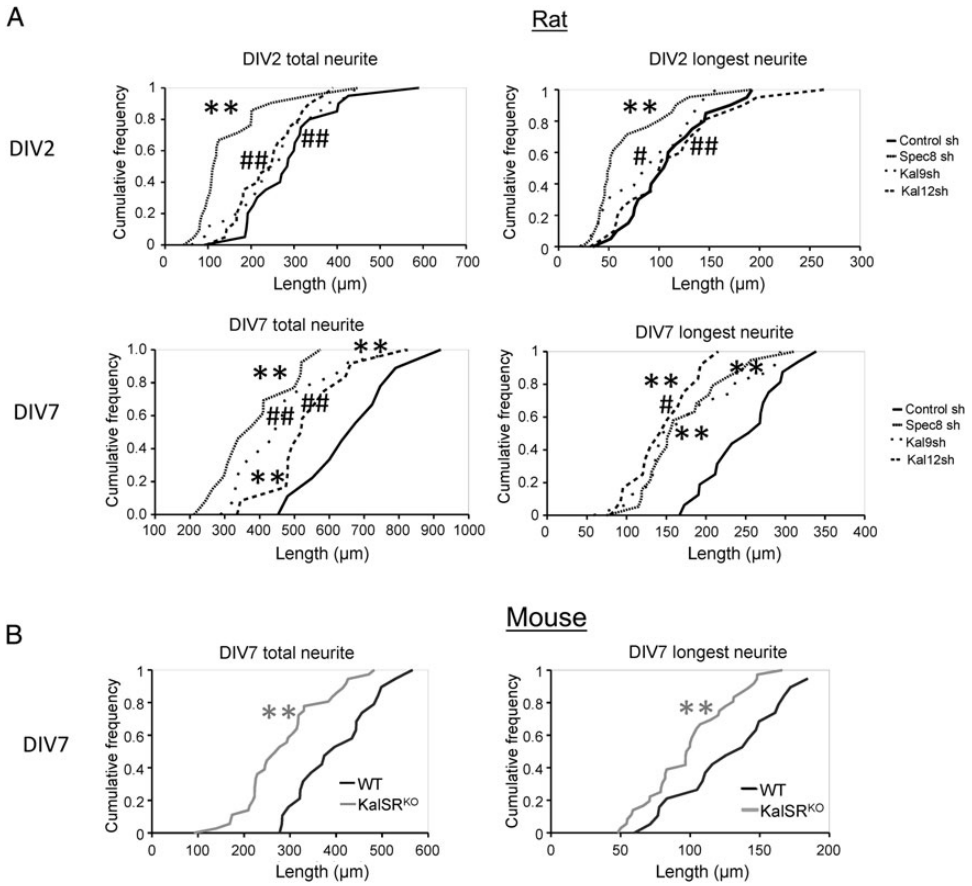

Figure 7. Kolmogorov–Smirnov analysis of cumulative distribution plots for total neurite and longest neurite length. Data for rat hippocampal neurons (*A*) and mouse cortical neurons (*B*) were obtained as described in Figures 4 and 6. Total neurite length and longest neurite length were evaluated at DIV2 and DIV7 (for shRNA-expressing rat hippocampal neurons) or at DIV7 (for WT and KalSR^{KO} cortical neurons); 15–27 neurons per group were measured. $^{**}P < 0.01$ to control shRNA or to WT; $^{\#}P < 0.05$, $^{\#\#}P < 0.01$ to Spec8 shRNA.

the KalGEF^{KO} mouse model, Xie et al. (2010) reported that dendritic spine density, dendritic branching, dendritic length, and complexity decreased in cortical neuronal cultures at DIV28, when Kal7 becomes the predominant isoform, while there were no significant changes found for hippocampal cultures at DIV28, yielding the conclusion that hippocampal neurons are more adaptive or resilient than cortical neurons, when Kalirin is ablated (Xie et al. 2011). Our data instead point to very similar effects in the early postnatal development of cultured hippocampal and cortical neurons deprived of Kalirin using shRNAs, genetic ablation, and pharmacological blockade (Figs 4, 5, and 7), which parallel the morphological defects seen in KalSR^{KO} cortical neurons in vivo (Fig. 2). The previous understanding of Kal9 and Kal12 functions was entirely based on overexpression studies (Penzes et al. 2001; May et al. 2002), which do not always accurately reflect normal physiological function. We found that expression of Kal9GFP rescued the decrease in neurite number and branching observed in neurons expressing Kal9 shRNA or Kal12 shRNA, but neurons expressing Kal9GFP in the absence of any detectable amount of shRNA resembled control (Scr) shRNA-expressing neurons. Examination of additional parameters in neurons expressing different doses of Kal9 and Kal12 will be needed to distinguish the actions of Kal9 and Kal12.

The effects of Z62954982 and ITX3 were quite similar, identifying the GEF1 domains of *Kalrn* and/or *Trio* as the key Rho GEFs. ITX3 treatment mimicked the *Kalrn* knockdown (shRNA) and genetic knockout phenotypes (Fig. 4 and 5), confirming the critical role of Kal GEF1. The application of Z62954983 or ITX3 to KalSR^{KO} neurons caused no morphological changes, demonstrating the dominant role of Kalirin among other Rho GEFs in early neuronal development. With the pharmacological tools available, it is not possible to determine whether Rac1 and RhoG both participate in the responses observed. The Rac1 residues targeted in the design of Z62954982 are shared by RhoG, leading to the expectation that activation of both Rho proteins will be inhibited by this compound (Ferri et al. 2009). RhoG is a far better substrate for the GEF1 domain of Kalirin than Rac1 (Jaiswal et al. 2013), but little is currently known about the sites or levels of expression of these 2 Rho proteins during development. While Rac1 and RhoG share some downstream targets, others are unique to Rac1 or to RhoG (Wennerberg et al. 2002). The published data on RhoG do not come to a consensus, with some reports arguing that RhoG reduces both axonal and dendritic tree complexity in vivo and in vitro (Franke et al. 2012), while other reports conclude that RhoG promotes spine morphogenesis (Kim et al. 2011). Further studies will be required to distinguish the roles of Rac1 and RhoG activation by endogenous Kalirin.

The distinctly different expression patterns of *Kalrn* and *Trio*, coupled with different phenotypes observed in mice

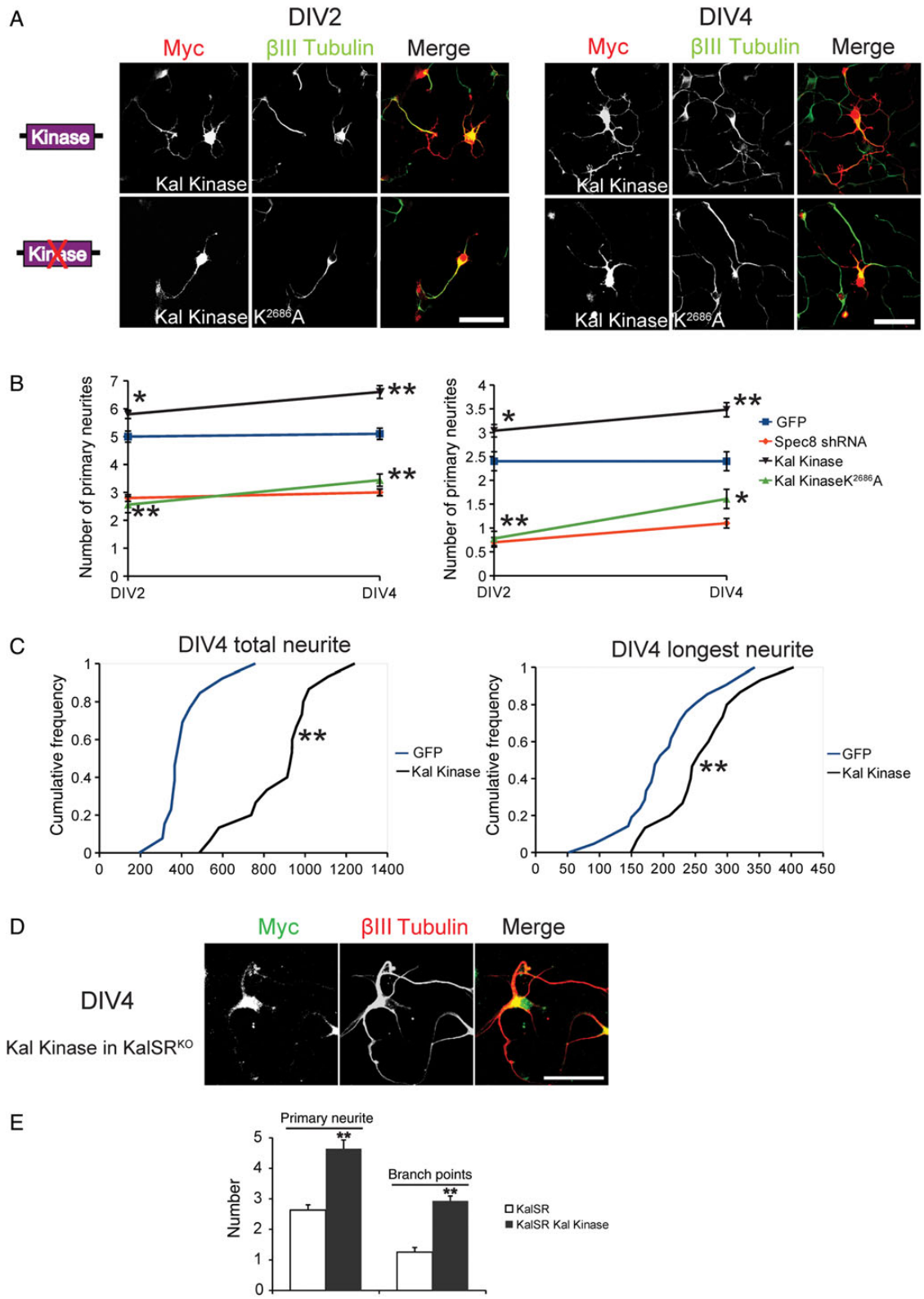

Figure 8. Active Kal Kinase domain promotes neurite growth and branching. (*A*) Examples of rat hippocampal neurons transfected at the time of plating with vector encoding mycKal Kinase or mycKal Kinase $K^{2686}A$; cultures were fixed at DIV2 and DIV4 and visualized by staining with antisera to myc and βIII tubulin. Scale bar: 50 μm. (*B*) The number of primary neurites and branch points was quantified as described above. Spec8 shRNA numbers are repeated from Figure 6. Control group, neurons expressing GFP; 4 separate experiments were performed and 6–12 neurons per group per experiment were analyzed. $*P < 0.05$, $**P < 0.01$. (*C*) Kolmogorov–Smirnov analysis of cumulative distribution plots of total neurite length and longest neurite at DIV4 for neurons expressing Kal Kinase or GFP. $**P < 0.01$. (*D*) Representative images of $KalSR^{KO}$ neurons transfected at the time of plating with vector encoding mycKal Kinase; cultures were fixed at DIV4 and stained with myc and βIII tubulin. Scale bar: 50 μm. (*E*) Numbers of primary neurites and branch points were quantified in $KalSR^{KO}$ neurons transfected with Kal Kinase.

lacking *Kalrn* and *Trio*, lead to the conclusion that these dual Rho GEFs fulfill different functions in mammals (Ma et al. 2005; McPherson et al. 2005; Peng et al. 2010; Miller et al. 2013; Wu et al. 2013). Although much remains to be learned about the distinct roles of the *Kalrn* and *Trio* genes, our initial studies indicate that *Trio* opposes the effects of *Kalrn* on neurite outgrowth and branching in early development (Yan *et al*. unpublished data).

Kal Kinase Is Involved in Neurite Development

The single *Kalrn/Trio* orthologue in invertebrates (*Unc-73*; *dTrio*) also undergoes extensive alternative splicing, but in *Drosophila* and in *C. elegans* none of the splice variants includes a kinase domain (Steven et al. 1998; Awasaki et al. 2000; Bateman et al. 2000). Kal9 and Trio-9 most closely resemble the longest isoforms of *Drosophila* Trio and *C. elegans* Unc-73. Both Kal12 and full-length Trio include a kinase domain (Debant et al. 1996; Johnson et al. 2000; McPherson et al. 2005), suggesting a unique role for this domain in higher organisms. Our data are the first to identify a role for the kinase domain of *Kalrn*, which promotes neurite growth independent of endogenous Kalirin. A member of the calcium/calmodulin-dependent protein kinase arm of the kinome, the sequence of Kal Kinase, is most closely related to that of Trio Kinase, the death-associated protein kinases, and several myosin light chain kinases. Autophosphorylation of Kal Kinase was detected in an in vitro kinase assay (Kawai et al. 1999), but no other substrate has been identified. Expression of the Kal Kinase domain (lacking the Ig and FnIII domains) resulted in increased neurite outgrowth and branching. The dominant negative effect of expressing what is expected to be a catalytically inactive Kal Kinase domain on neurite number and branch point formation makes the search for its substrates worthwhile (Fig. 8).

Dendritic Arbor Formation and Axonal Polarity

Prior to the elaboration of dendrites, axon–dendritic polarization is established, followed by morphological and functional specification of dendritic and axonal compartments. These two steps are regulated by different pathways (Barnes and Polleux 2009; Puram and Bonni 2013). We used conventional E18 rat hippocampal cultures, so the majority of the cells are postmitotic neurons and neuronal polarization would have been established in vivo, before dissociation and plating (Barnes and Polleux 2009). In culture, we are observing the repolarization of these neurons, and knocking down both endogenous Kal9 and Kal12 did not impair axon polarization when assessed at DIV4 or DIV7.

Changes in dendrite branching and in axonal outgrowth were observed in the absence of Kal9/Kal12. The Rho GTPases are key regulators of the cytoskeleton in both dendrite growth and arborization (Luo 2000a, 2000b; Hayashi-Takagi et al. 2010; Peng et al. 2010). Rac1 appears to drive dendrite elaboration (Redmond and Ghosh 2001; Jan and Jan 2010), and our study confirmed the importance of Kal GEF1 activity in dendrite morphogenesis. Both neurite length and branching were reduced in the absence of endogenous Kal9/Kal12. These 2 parameters are closely related, since shorter neurites, with less exposure to cell-extrinsic growth cues, may form fewer branch points.

Neither *C. elegans UNC-73* nor *D. melanogaster dTrio* encodes an isoform similar to Kal7, with its post synaptic density protein [PSD95], Drosophila disc large tumor suppressor [Dlg1], and zonula occludens-1 protein [zo-1]-binding motif, or an isoform similar to Kal12, with its kinase domain. Kal7, which localizes to the PSD and has no Trio homolog, plays an essential role in the formation and function of excitatory synapses on dendritic spines (Ma et al. 2003, 2008), a specialization not found on the dendrites of *C. elegans* or *D. melanogaster* neurons (Lamprecht 2014). Expression of exogenous Kal Kinase had a much greater effect on total neurite length than on the length of the longest neurite (axon; Fig. 8*C*), suggesting that the kinase domain may also have a special role in dendritic morphogenesis.

Association with Cognitive Deficits in Adult Animals

The simplified dendritic arbor observed in KalSR^{KO} animals and loss of dendrite branches in KalSR^{KO} cultures in early development may provide a link to the impairment of cognitive functions observed in adult Kalirin knockout animals (Xie et al. 2011; Mandela et al. 2012). The deficits include blunted anxiety-like behavior and impaired fear-based learning, which might result from defects in dendrite morphogenesis and maintenance. Accumulating evidence suggests that alterations in dendrite morphology, including dendrite branching patterns, fragmentation of dendrites, and loss of dendrite branching, contribute to neurological and neurodevelopmental disorders such as anxiety and schizophrenia (Eiland and McEwen 2012; Kulkarni and Firestein 2012).

Significance

Our observations may provide useful insights into the pathophysiology of schizophrenia and other neurodevelopmental or neurodegenerative disorders. *Kalrn* is strongly associated with schizophrenia in human studies (Hill et al. 2006; Kushima et al. 2012; Rubio et al. 2012). Previous studies focused on changes in *Kalrn* expression underlying dendritic spine loss, an event that happens later in development in the cortices (Hill et al. 2006; Rubio et al. 2012). Our study is the first to identify deficits in the dendritic arbor due to the absence of Kal9 or Kal12 in early development, before dendritic spine formation, and is potentially relevant to the molecular mechanisms underlying the development of schizophrenia in children. Defects in dendritic arbor structure were observed in hippocampal neurons lacking endogenous Kal9/Kal12, a finding that is consistent with the observation that schizophrenia patients demonstrating positive symptoms exhibit decreased dendritic branching and spine numbers in hippocampus (Kulkarni and Firestein 2012). Genome-wide association studies detected a significant association between schizophrenia and the *Kalrn* P^{2255}T mutation (Kushima et al. 2012), which affects Kal9 and Kal12, but not Kal7. This mutation, located between the GEF2 and SH3 domains, may affect the phosphorylation status of Kal9/Kal12. Kal7 is a substrate for multiple protein kinases, and Kal7 isolated from mouse brain is heavily phosphorylated (Kiraly et al. 2011). The phosphorylation state of Kal9/Kal12 has not yet been examined. Our data on the functional consequences of losing Kal9 and/or Kal12 in early development may point to the development of therapeutic interventions to restore abnormal signal transduction in schizophrenia in both cortex and hippocampus.

Authors' Contributions

Y.Y., B.A.E., and R.E.M. designed research, performed research, analyzed data, and wrote the paper.

Funding

This work was supported by grants from the National Institute of Drug Abuse (DA015464 and DA023082) and the National Institute of Diabetes, Digestive and Kidney Diseases (DK032948), both in the National Institutes of Health, and by the Janice and Rodney Reynolds Endowment and the Scoville Endowment.

Notes

We thank Yanping Wang and Darlene D'Amato for incomparable technical support and Dr Prashant Mandela for providing KalSR^{KO} breeders. *Conflict of Interest*: None declared.

References

Adams BD, Claffey KP, White BA. 2009. Argonaute-2 expression is regulated by epidermal growth factor receptor and mitogen-activated protein kinase signaling and correlates with a transformed phenotype in breast cancer cells. Endocrinology. 150:14–23.

Awasaki T, Saito M, Sone M, Suzuki E, Sakai R, Ito K, Hama C. 2000. The Drosophila trio plays an essential role in patterning of axons by regulating their directional extension. Neuron. 26:119–131.

Barnes AP, Polleux F. 2009. Establishment of axon-dendrite polarity in developing neurons. Annu Rev Neurosci. 32:347–381.

Bateman J, Shu H, Van Vactor D. 2000. The guanine nucleotide exchange factor trio mediates axonal development in the Drosophila embryo. Neuron. 26:93–106.

Bouquier N, Vignal E, Charrasse S, Weill M, Schmidt S, Leonetti JP, Blangy A, Fort P. 2009. A cell active chemical GEF inhibitor selectively targets the Trio/RhoG/Rac1 signaling pathway. Chem Biol. 16:657–666.

Caldwell BD, Darlington DN, Penzes P, Johnson RC, Eipper BA, Mains RE. 1999. The novel kinase peptidylglycine alpha-amidating monooxygenase cytosolic interactor protein 2 interacts with the cytosolic routing determinants of the peptide processing enzyme peptidylglycine alpha-amidating monooxygenase. J Biol Chem. 274: 34646–34656.

Craig AM, Banker G. 1994. Neuronal polarity. Annu Rev Neurosci. 17:267–310.

Debant A, Serra-Pages C, Seipel K, O'Brien S, Tang M, Park SH, Streuli M. 1996. The multidomain protein Trio binds the LAR transmembrane tyrosine phosphatase, contains a protein kinase domain, and has separate rac-specific and rho-specific guanine nucleotide exchange factor domains. Proc Natl Acad Sci USA. 93:5466–5471.

Dotti CG, Sullivan CA, Banker GA. 1988. The establishment of polarity by hippocampal neurons in culture. J Neurosci. 8:1454–1468.

Eiland L, McEwen BS. 2012. Early life stress followed by subsequent adult chronic stress potentiates anxiety and blunts hippocampal structural remodeling. Hippocampus. 22:82–91.

Ferri N, Corsini A, Bottino P, Clerici F, Contini A. 2009. Virtual screening approach for the identification of new Rac1 inhibitors. J Med Chem. 52:4087–4090.

Francone VP, Ifrim MF, Rajagopal C, Leddy CJ, Wang Y, Carson JH, Mains RE, Eipper BA. 2010. Signaling from the secretory granule to the nucleus: Uhmk1 and PAM. Mol Endocrinol. 24:1543–1558.

Franke K, Otto W, Johannes S, Baumgart J, Nitsch R, Schumacher S. 2012. miR-124-regulated RhoG reduces neuronal process complexity via ELMO/Dock180/Rac1 and Cdc42 signalling. EMBO J. 31:2908–2921.

Hayashi-Takagi A, Takaki M, Graziane N, Seshadri S, Murdoch H, Dunlop AJ, Makino Y, Seshadri AJ, Ishizuka K, Srivastava DP et al. 2010. Disrupted-in-Schizophrenia 1 (DISC1) regulates spines of the glutamate synapse via Rac1. Nat Neurosci. 13:327–332.

Hill JJ, Hashimoto T, Lewis DA. 2006. Molecular mechanisms contributing to dendritic spine alterations in the prefrontal cortex of subjects with schizophrenia. Mol Psychiatry. 11:557–566.

Huh KH, Wenthold RJ. 1999. Turnover analysis of glutamate receptors identifies a rapidly degraded pool of the *N*-methyl-D-aspartate receptor subunit, NR1, in cultured cerebellar granule cells. J Biol Chem. 274:151–157.

Jaffe AB, Hall A. 2005. Rho GTPases: biochemistry and biology. Annu Rev Cell Dev Biol. 21:247–269.

Jaiswal M, Dvorsky R, Ahmadian MR. 2013. Deciphering the molecular and functional basis of Dbl family proteins: a novel systematic approach toward classification of selective activation of the Rho family proteins. J Biol Chem. 288:4486–4500.

Jan YN, Jan LY. 2010. Branching out: mechanisms of dendritic arborization. Nat Rev Neurosci. 11:316–328.

Johnson RC, Penzes P, Eipper BA, Mains RE. 2000. Isoforms of kalirin, a neuronal Dbl family member, generated through use of different 5′- and 3′-ends along with an internal translational initiation site. J Biol Chem. 275:19324–19333.

Kawai T, Sanjo H, Akira S. 1999. Duet is a novel serine/threonine kinase with Dbl-Homology (DH) and Pleckstrin-Homology (PH) domains. Gene. 227:249–255.

Kim JY, Oh MH, Bernard LP, Macara IG, Zhang H. 2011. The RhoG/ELMO1/Dock180 signaling module is required for spine morphogenesis in hippocampal neurons. J Biol Chem. 286:37615–37624.

Kiraly DD, Ma XM, Mazzone CM, Xin X, Mains RE, Eipper BA. 2010. Behavioral and morphological responses to cocaine require kalirin7. Biol Psychiatry. 68:249–255.

Kiraly DD, Stone KL, Colangelo CM, Abbott T, Wang Y, Mains RE, Eipper BA. 2011. Identification of kalirin-7 as a potential post-synaptic density signaling hub. J Proteome Res. 10:2828–2841.

Konur S, Ghosh A. 2005. Calcium signaling and the control of dendritic development. Neuron. 46:401–405.

Kulkarni VA, Firestein BL. 2012. The dendritic tree and brain disorders. Mol Cell Neurosci. 50:10–20.

Kushima I, Nakamura Y, Aleksic B, Ikeda M, Ito Y, Shiino T, Okochi T, Fukuo Y, Ujike H, Suzuki M et al. 2012. Resequencing and association analysis of the KALRN and EPHB1 genes and their contribution to schizophrenia susceptibility. Schizophr Bull. 38:552–560.

Lamprecht R. 2014. The actin cytoskeleton in memory formation. Prog Neurobiol. 117:1–19.

Luo L. 2000a. Rho GTPases in neuronal morphogenesis. Nat Rev Neurosci. 1:173–180.

Luo L. 2000b. Trio quartet in *D.* (*melanogaster*). Neuron. 26:1–2.

Ma XM, Huang JP, Eipper BA, Mains RE. 2005. Expression of Trio, a member of the Dbl family of Rho GEFs in the developing rat brain. J Comp Neurol. 482:333–348.

Ma XM, Huang J, Wang Y, Eipper BA, Mains RE. 2003. Kalirin, a multifunctional Rho guanine nucleotide exchange factor, is necessary for maintenance of hippocampal pyramidal neuron dendrites and dendritic spines. J Neurosci. 23:10593–10603.

Ma XM, Wang Y, Ferraro F, Mains RE, Eipper BA. 2008. Kalirin-7 is an essential component of both shaft and spine excitatory synapses in hippocampal interneurons. J Neurosci. 28:711–724.

Mandela P, Yankova M, Conti LH, Ma XM, Grady J, Eipper BA, Mains RE. 2012. Kalrn plays key roles within and outside of the nervous system. BMC Neurosci. 13:136.

May V, Schiller MR, Eipper BA, Mains RE. 2002. Kalirin Dbl-homology guanine nucleotide exchange factor 1 domain initiates new axon outgrowths via RhoG-mediated mechanisms. J Neurosci. 22:6980–6990.

McPherson CE, Eipper BA, Mains RE. 2002. Genomic organization and differential expression of Kalirin isoforms. Gene. 284:41–51.

McPherson CE, Eipper BA, Mains RE. 2005. Multiple novel isoforms of Trio are expressed in the developing rat brain. Gene. 347:125–135.

Miller MB, Yan Y, Eipper BA, Mains RE. 2013. Neuronal Rho GEFs in synaptic physiology and behavior. Neuroscientist. 19:255–273.

Morales-Corraliza J, Mazzella MJ, Berger JD, Diaz NS, Choi JH, Levy E, Matsuoka Y, Planel E, Mathews PM. 2009. In vivo turnover of tau

and APP metabolites in the brains of wild-type and Tg2576 mice: greater stability of sAPP in the beta-amyloid depositing mice. PLoS ONE. 4:e7134.
Nakayama AY, Harms MB, Luo L. 2000. Small GTPases Rac and Rho in the maintenance of dendritic spines and branches in hippocampal pyramidal neurons. J Neurosci. 20:5329–5338.
Pardo CA, Eberhart CG. 2007. The neurobiology of autism. Brain Pathol. 17:434–447.
Peng YJ, He WQ, Tang J, Tao T, Chen C, Gao YQ, Zhang WC, He XY, Dai YY, Zhu NC et al. 2010. Trio is a key guanine nucleotide exchange factor coordinating regulation of the migration and morphogenesis of granule cells in the developing cerebellum. J Biol Chem. 285:24834–24844.
Penzes P, Johnson RC, Kambampati V, Mains RE, Eipper BA. 2001. Distinct roles for the two Rho GDP/GTP exchange factor domains of kalirin in regulation of neurite growth and neuronal morphology. J Neurosci. 21:8426–8434.
Petreanu L, Mao T, Sternson SM, Svoboda K. 2009. The subcellular organization of neocortical excitatory connections. Nature. 457:1142–1145.
Puram SV, Bonni A. 2013. Cell-intrinsic drivers of dendrite morphogenesis. Development. 140:4657–4671.
Redmond L, Ghosh A. 2001. The role of Notch and Rho GTPase signaling in the control of dendritic development. Curr Opin Neurobiol. 11:111–117.
Rubio MD, Haroutunian V, Meador-Woodruff JH. 2012. Abnormalities of the Duo/Ras-related C3 botulinum toxin substrate 1/p21-activated kinase 1 pathway drive myosin light chain phosphorylation in frontal cortex in schizophrenia. Biol Psychiatry. 71:906–914.
Schiller MR, Ferraro F, Wang Y, Ma XM, McPherson CE, Sobota JA, Schiller NI, Mains RE, Eipper BA. 2008. Autonomous functions for the Sec14p/spectrin-repeat region of Kalirin. Exp Cell Res. 314:2674–2691.
Shen HW, Toda S, Moussawi K, Bouknight A, Zahm DS, Kalivas PW. 2009. Altered dendritic spine plasticity in cocaine-withdrawn rats. J Neurosci. 29:2876–2884.
Sobota JA, Back N, Eipper BA, Mains RE. 2009. Inhibitors of the V0 subunit of the vacuolar H^+-ATPase prevent segregation of lysosomal- and secretory-pathway proteins. J Cell Sci. 122:3542–3553.
Sommer JE, Budreck EC. 2009. Kalirin-7: linking spine plasticity and behavior. J Neurosci. 29:5367–5369.
Steven R, Kubiseski TJ, Zheng H, Kulkarni S, Mancillas J, Ruiz Morales A, Hogue CW, Pawson T, Culotti J. 1998. UNC-73 activates the Rac GTPase and is required for cell and growth cone migrations in *C. elegans*. Cell. 92:785–795.
Tada T, Sheng M. 2006. Molecular mechanisms of dendritic spine morphogenesis. Curr Opin Neurobiol. 16:95–101.
Van Maldergem L, Hou Q, Kalscheuer VM, Rio M, Doco-Fenzy M, Medeira A, de Brouwer AP, Cabrol C, Haas SA, Cacciagli P et al. 2013. Loss of function of KIAA2022 causes mild to severe intellectual disability with an autism spectrum disorder and impairs neurite outgrowth. Hum Mol Genet. 22:3306–3314.
Wennerberg K, Ellerbroek SM, Liu RY, Karnoub AE, Burridge K, Der CJ. 2002. RhoG signals in parallel with Rac1 and Cdc42. J Biol Chem. 277:47810–47817.
Wong RO, Ghosh A. 2002. Activity-dependent regulation of dendritic growth and patterning. Nat Rev Neurosci. 3:803–812.
Wu JH, Fanaroff AC, Sharma KC, Smith LS, Brian L, Eipper BA, Mains RE, Freedman NJ, Zhang L. 2013. Kalirin promotes neointimal hyperplasia by activating Rac in smooth muscle cells. Arterioscler Thromb Vasc Biol. 33:702–708.
Xie Z, Cahill ME, Penzes P. 2010. Kalirin loss results in cortical morphological alterations. Mol Cell Neurosci. 43:81–89.
Xie Z, Cahill ME, Radulovic J, Wang J, Campbell SL, Miller CA, Sweatt JD, Penzes P. 2011. Hippocampal phenotypes in kalirin-deficient mice. Mol Cell Neurosci. 46:45–54.
Xu B, Hsu PK, Stark KL, Karayiorgou M, Gogos JA. 2013. Derepression of a neuronal inhibitor due to miRNA dysregulation in a schizophrenia-related microdeletion. Cell. 152:262–275.
Yan Y, Zhou X, Pan Z, Ma J, Waschek JA, DiCicco-Bloom E. 2013. Pro- and anti-mitogenic actions of pituitary adenylate cyclase-activating polypeptide in developing cerebral cortex: potential mediation by developmental switch of PAC1 receptor mRNA isoforms. J Neurosci. 33:3865–3878.
Zhou D, Lambert S, Malen PL, Carpenter S, Boland LM, Bennett V. 1998. AnkyrinG is required for clustering of voltage-gated Na channels at axon initial segments and for normal action potential firing. J Cell Biol. 143:1295–1304.